JACS
JOURNAL OF THE AMERICAN CHEMICAL SOCIETY
pubs.acs.org/JACS

Article

Excited-State (Anti)Aromaticity Explains Why Azulene Disobeys Kasha's Rule

David Dunlop, Lucie Ludvíková, Ambar Banerjee, Henrik Ottosson,* and Tomáš Slanina*

Cite This: J. Am. Chem. Soc. 2023, 145, 21569−21575

Read Online

ACCESS | Metrics & More | Article Recommendations | Supporting Information

ABSTRACT: Fluorescence exclusively occurs from the lowest excited state of a given multiplicity according to Kasha's rule. However, this rule is not obeyed by a handful of anti-Kasha fluorophores whose underlying mechanism is still understood merely on a phenomenological basis. This lack of understanding prevents the rational design and property-tuning of anti-Kasha fluorophores. Here, we propose a model explaining the photophysical properties of an archetypal anti-Kasha fluorophore, azulene, based on its ground- and excited-state (anti)aromaticity. We derived our model from a detailed analysis of the electronic structure of the ground singlet, first excited triplet, and quintet states and of the first and second excited singlet states using the perturbational molecular orbital theory and quantum-chemical aromaticity indices. Our model reveals that the anti-Kasha properties of azulene and its derivatives result from (i) the contrasting (anti)aromaticity of its first and second singlet excited states (S_1 and S_2, respectively) and (ii) an easily accessible antiaromaticity relief pathway of the S_1 state. This explanation of the fundamental cause of anti-Kasha behavior may pave the way for new classes of anti-Kasha fluorophores and materials with long-lived, high-energy excited states.

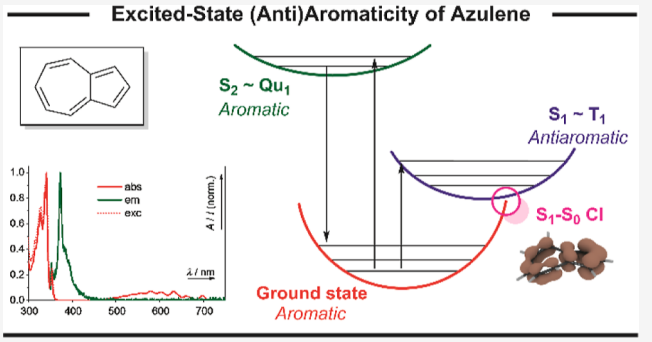

1. INTRODUCTION

In 1959, Michael Kasha postulated that, in single molecules, "the emitting level of a given multiplicity is the lowest excited level of that multiplicity".[1] Since then, however, Kasha's rule has been broken by a number of molecules known as anti-Kasha (also non-Kasha) fluorophores.[2−4] Among them, one fluorophore stands out for exclusively emitting from the second singlet excited state (S_2) as the archetype of anti-Kasha fluorophores, azulene.[5]

Azulene's anti-Kasha behavior is particularly robust under structural perturbations. Binsch et al. tried to quell the anti-Kasha properties of azulene through multiple synthetic strategies, including annellation, symmetry lowering, substitution by heavy atoms, and addition of a "loose bolt" substituent (Figure 1A), albeit to no avail.[6] All approaches failed to induce the first singlet excited state (S_1) emission of the azulene derivatives.

Based on Longuet-Higgins and Beer's hypothesis according to which the anomalous emission of azulene results from its large S_2−S_1 gap (~14,000 cm^{-1}),[5] Murata et al. followed a more systematic approach to reduce the S_2−S_1 gap by extensive substitution of the azulene scaffold (Figure 1B).[7] They were able to increase the rate of S_2−S_1 internal conversion, thereby reducing the quantum yield of the S_2 emission. Yet, even in later studies, despite the increased IC rate, no S_1 emission was observed in any azulene derivative at room temperature.[8−15]

The anomalous photophysical properties of azulene and its derivatives prompted further research efforts to uncover their underlying mechanism, leading to the following, now well-established explanations: (i) the large S_2−S_1 gap of azulene results in a low rate of IC from S_2, which in turn leads to a high yield of S_2 emission,[5,7,10] and (ii) the S_1 of azulene rapidly decays by a S_1−S_0 conical intersection,[18] located near the S_1 minimum energy geometry, thereby accounting for the absence of S_1 emission. Notwithstanding these efforts, no structure−property relationship was provided to explain the anti-Kasha behavior of azulene. In fact, the description of azulene's anti-Kasha behavior has long remained insufficient to guide any attempt at rational molecular design and anti-Kasha property tuning, a shortcoming that we shall overcome herein.

Azulene is a 10π-aromatic fused bicyclic hydrocarbon with no substituents or heteroatoms; therefore, its photophysical phenomena must be a manifestation of its π-electron configuration. Cyclic, π-conjugated molecules can be described as aromatic or antiaromatic in their ground and excited

Received: July 17, 2023
Published: September 13, 2023

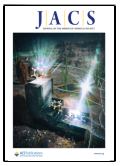

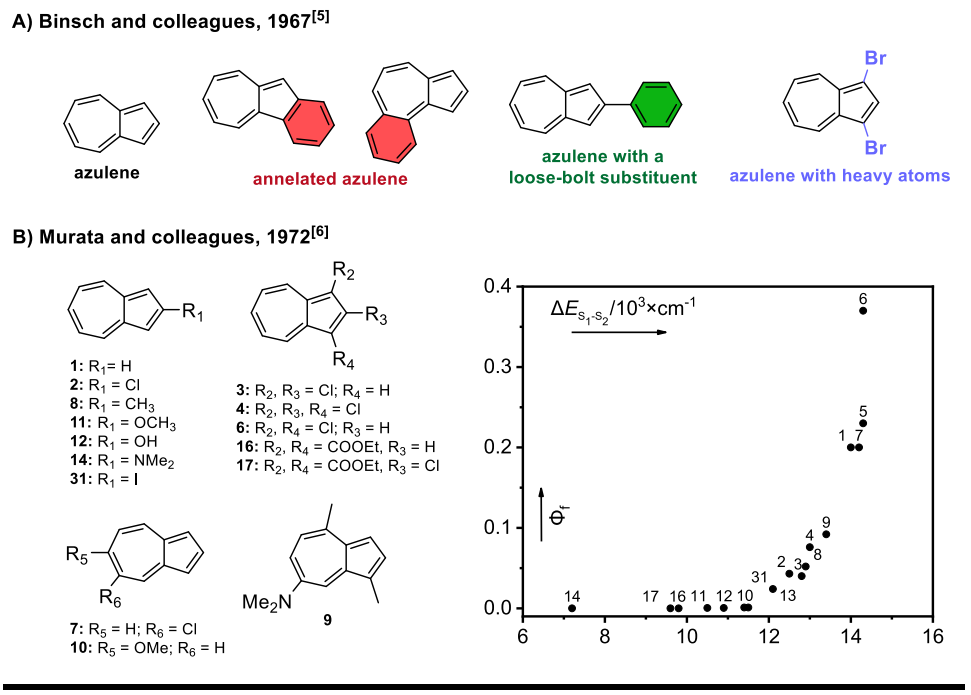

Figure 1. Examples of anti-Kasha azulene derivatives: (A) substituent effects explored by Binsch et al.,[6] (B) derivatives (numbered as in the original publication) explored by Murata et al. (left) and a plot of fluorescence quantum yields as a function of S_1-S_2 gap (right).[7]

states.[19−24] Among other characteristics, these descriptors indicate whether their π-electron configuration in a given electronic state is stabilizing or destabilizing, respectively. Accordingly, we hypothesized that the anti-Kasha behavior of azulene could be related to the (anti)aromatic character of S_1 and S_2. Such a relationship between excited-state (anti)-aromaticity and anti-Kasha behavior may explain how the electronic structure of azulene leads to its anti-Kasha behavior, thus providing key mechanistic insights into anti-Kasha fluorophores.

2. RESULTS AND DISCUSSION

To understand how the electronic structure of azulene leads to its anti-Kasha behavior, we analyzed its ground- and excited-state (anti)aromaticity in increasing order of complexity. The ground singlet state (S_0) and first-excited triplet state (T_1) of small conjugated cyclic hydrocarbons typically show contrasting aromaticity/antiaromaticity, as per Hückel's and Baird's rules.[20] Moreover, the aromaticity of the first excited quintet state (Qu_1) of azulene has been previously reported.[25,26] Hence, we computationally investigated the S_0, T_1, and Qu_1 to model the (anti)aromatic character of azulene in the lowest states of each multiplicity. Subsequently, we compared their electronic structures and various aromaticity indices (Section S5) with those of S_1 and S_2, which account for the anti-Kasha behavior of azulene. This approach enabled us to establish the relationship between the anti-Kasha behavior of azulene and its excited-state (anti)aromaticity.

Ground state azulene is a Hückel 10π-aromatic molecule, as shown by all calculated aromaticity indices (Figure 2 and Chapter S5.1). Yet, only when comparing the calculated aromaticity indices of all possible delocalization circuits within its molecular geometry (Figure S6) do we find that the aromaticity of azulene originates from the delocalization along

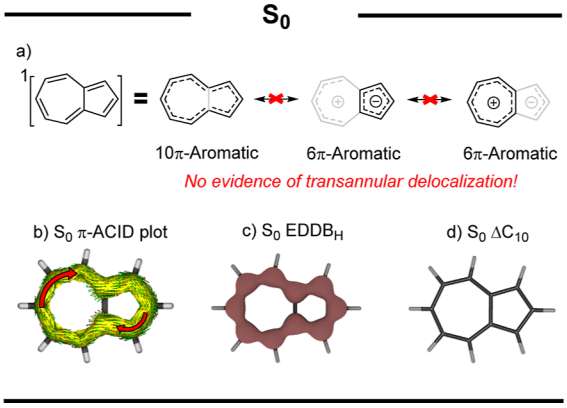

Figure 2. Summary of the results of S_0 azulene; (a) important resonance structures, (b) S_0 π-ACID plot (Figure S35), (c) S_0 $EDDB_H$, and (d) density of delocalized π-electrons in the transannular bond (ΔC_{10}), which corresponds to the density of 0.02 electrons (amounting to virtually no delocalization through the transannular bond).

its perimeter. The calculated delocalization indices [aromatic fluctuation (FLU), multicenter delocalization (MCI), and electron density of delocalized bonds (EDDB)] indicate (Table S1) that most of the delocalized 10π-electron density is situated along the perimeter of azulene (cyclodecapentaenyl circuit). Conversely, delocalization circuits involving the transannular bond (cyclopentadienyl and cycloheptatrienyl) exhibit poor π-electron delocalization (Figure 2 and Table S1). By calculating $EDDB_P$ electron counts (Table S2), we quantified the electron delocalization within the transannular bond of azulene (ΔC_{10}). This bond exhibited only a negligible contribution, 0.02 electrons, to the global delocalized electron density of azulene (Figure 2). The virtual absence of ground-

https://doi.org/10.1021/jacs.3c07625
J. Am. Chem. Soc. 2023, 145, 21569−21575

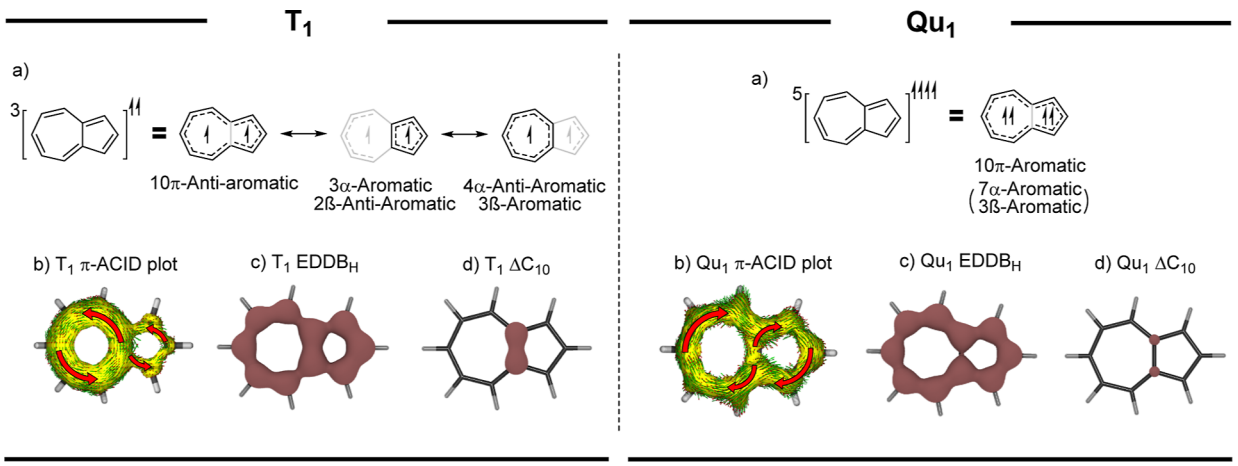

Figure 3. Summary of the results of T_1 and Qu_1 azulene; (a) most prevalent resonance structures, (b) π-ACID plots (Figures S36 and S37), (c) $EDDB_H$, and (d) density of delocalized π-electrons in the transannular bond (ΔC_{10}).

state transannular delocalization in azulene corresponds to its unusually long transannular bond of approximately 1.5 Å.[27]

The 10π-aromaticity of azulene was predicted in previous studies.[26,28] However, the relevance of this finding has been largely overlooked. For example, the permanent dipole moment of azulene is usually explained by resonance structures that invoke delocalization through the transannular bond,[29] but these resonance structures do not significantly contribute to the net electronic structure of azulene (Figure 2a), as evidenced by the negligible ΔC_{10} value. As a case in point, we found that homoazulene,[30] the homoannelated counterpart of azulene without a conjugated transannular bond, has a similar permanent dipole moment (Chapter S13.1). Furthermore, in contrast to many other polycyclic aromatic hydrocarbons (PAH), such as the isoelectronic naphthalene (Chapter S13.2), which is known to favor the formation of multiple, 6π-aromatic rings,[31,32] azulene's S_0 electronic structure resembles a single 10π-aromatic ring. Therefore, in the ground state, the bicyclic molecular geometry of azulene should be treated as a single 10π-aromatic hydrocarbon rather than a PAH.

In the first triplet excited state, azulene follows Baird's rules[19] and is antiaromatic (Figure 3). This antiaromaticity is partly alleviated by transannular bond contraction. As a result, the delocalization decreases in the perimeter but increases in the cyclopentadienyl and cycloheptatrienyl circuits of azulene, as shown by our calculations (Table S5), and these circuits adopt the electronic structures of their corresponding cyclic radicals, as demonstrated by the EDDB (Chapter S12). The consequences of this enhanced geometric relaxation and the associated changes in the electronic structure of azulene can also be observed in the calculated isomerization stabilization energies (ISE) (Table S30), which are close to zero, or negative, for methylated isomers of T_1 azulene. Despite the extensive reorganization and significant loss of antiaromaticity, T_1 azulene remains, nevertheless, moderately antiaromatic.

The Qu_1 of azulene has never been observed experimentally. However, previous theoretical studies have indicated that Qu_1 azulene is aromatic.[25,26] Furthermore, our results showed that the aromaticity of Qu_1 originates primarily from the delocalization along its perimeter (Figure 3 and Table S9). The contrasting preferred electronic structures of T_1 and Qu_1 azulene are supported by both the perturbational molecular orbital (PMO) theory[28] (Chapter S3.1.1) and Mandado's rules[33] (Chapter S3.1.2).

The concepts developed based on the S_0, T_1, and Qu_1 azulene enabled us to evaluate the aromaticity of azulene in S_1 and S_2 (Figure 4). The complete active space self-consistent field (CASSCF) aromaticity indices (Table S13) indicated that the S_1 azulene is antiaromatic, whereas its S_2 is aromatic.

We investigated the (anti)aromaticity of S_1 and S_2 azulene further by calculating the magnetically induced current density (MICD) at the CASSCF(10,10) level.[34,35] We found that azulene in S_2, similarly to S_0, exhibited a diatropic ring current along its perimeter. Conversely, azulene in S_1 exhibited a paratropic ring current, localized primarily within the cyclopentadienyl and cycloheptatrienyl circuits (Figure 4B). The polarity of the MICD confirmed the antiaromaticity of azulene in S_1 and the aromaticity in S_2.

The S_1 antiaromaticity of azulene followed Baird's rules. Although Baird's rules were originally formulated only for molecules in T_1,[19] in many molecules, the rules can be applied to S_1 as well.[20] The similarity between the S_1 and T_1 azulene is indicated by the calculated energies, minimum energy molecular geometries, aromaticity indices, and EDDB values (Figure 4 and Chapter S5.4).

Our findings also explain the aromaticity of S_2 azulene. The root-optimized CASSCF(10,10) wave function of S_2 azulene has a significant multireference character (Figure 4 and Tables S18 and S19). The wave function attributed near-degenerate occupancy by unpaired electrons to HOMO − 1 and LUMO and to HOMO and LUMO + 1. This factor plays a key role in the S_2 aromaticity of azulene. The multireference character of S_2 azulene mimics the Qu_1 state by adopting a similar normalized π-orbital occupancy, in a relationship not unlike S_1−T_1. Consequently, the S_2 and Qu_1 states of azulene share a similar aromatic character.

In summary, S_1 azulene is antiaromatic, and its geometry relaxes significantly to alleviate its antiaromaticity, whereas S_2 azulene is aromatic, and its geometry does not relax significantly, thus preserving the energy gained upon excitation. Moreover, in antiaromatic S_1, azulene adopts a biradical electronic structure. The biradical electronic structure of S_1 azulene leads to spatial segregation of its two unpaired electrons into π and π^* orbitals. Thus, in S_1, azulene's unpaired electrons exhibit low interelectron repulsion, which contributes to its low S_1 energy (previously also described by Michl and Thulstrup).[36] In the aromatic S_2, conversely, the two unpaired electrons are delocalized within the azulene's perimeter circuit.

https://doi.org/10.1021/jacs.3c07625
J. Am. Chem. Soc. 2023, 145, 21569−21575

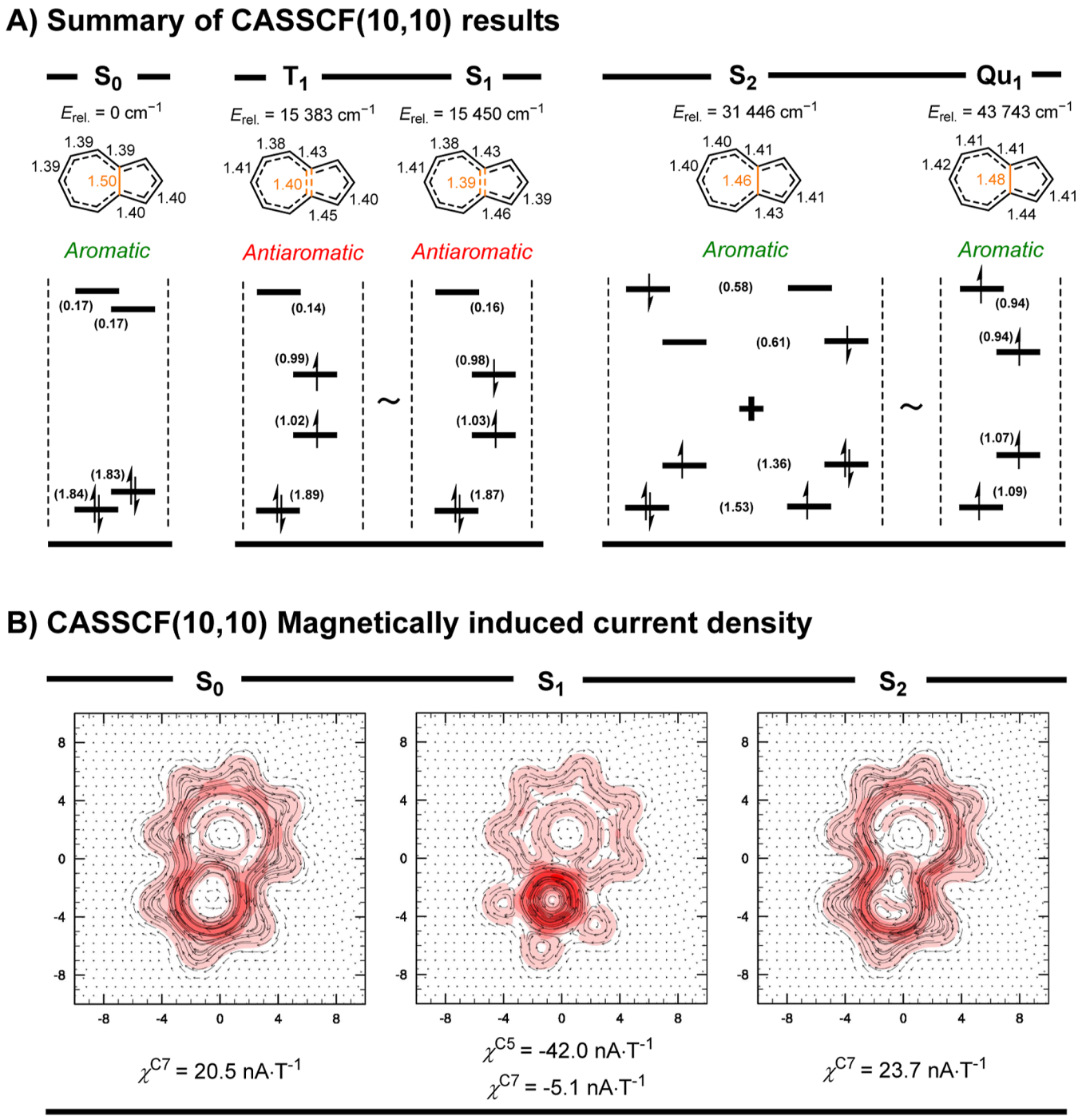

Figure 4. (A) Summary of calculated properties of the CASSCF(10,10) wave functions of the S_0, S_1, S_2, T_1, and Qu_1 of azulene, grouped by their shared aromaticity ($S_1 \sim T_1$, $S_2 \sim Qu_1$), including their (from top): relative energies in reference to the S_0 ($E_{rel.}$) which in case of S_1 (318 nm) and S_2 (647 nm) directly relate to the UV−vis absorption bands of azulene (see Figure 6B), bond lengths (C_{2V} symmetry), assigned aromatic character, canonicalized active-space natural MOs [reduced to (4,4) for clarity], their normalized occupancy (in brackets), and scheme of the dominant configuration(s). (B) CASSCF(10,10) MICD plot of azulene in S_0, S_1, and S_2, constructed 1 au above the molecular plane (for full resolution plots, see Figures S38−S40), and the numerically integrated ring current susceptibilities of the cyclopentadienyl (χ^{C5}) and cycloheptatrienyl (χ^{C7}) rings (for integration planes, see Figure S7).

Accordingly, in S_2 azulene, the unpaired electrons share a higher orbital overlap, resulting in higher interelectron repulsion. This contrast between the extent of geometric relaxation of azulene in S_1 and S_2 and the resulting difference in interelectron repulsion explains the large S_2-S_1 energy separation and, consequently, leads to a low rate of S_2-S_1 internal conversion (IC).

At this point, the absence of S_1 emission caused by the depletion of S_1 states via a S_1-S_0 conical intersection[18] remained unaddressed though. To account for this key feature of the anti-Kasha behavior of azulene, we optimized the S_1-S_0 conical intersection geometry and calculated the CASSCF aromaticity indices (Section S5.5), as previously performed for S_1 and S_2. In the optimized conical intersection geometry, S_1

https://doi.org/10.1021/jacs.3c07625
J. Am. Chem. Soc. 2023, 145, 21569−21575

azulene adopts the electronic structure of two acyclic radicals separated by a double bond (Figure 5), in turn increasing the overall energy. This increase is offset by subsequent nonradiative transition to the aromatic ground state (Table S1). As suggested by canonicalized active-space natural MO's (Figure 5c), at the CI geometry, azulene exhibits low HOMO−LUMO separation. This low separation favors the pairing of its two unpaired electrons (in S_1), thus providing a nonradiative pathway to S_0. Therefore, the conical intersection enables S_1 antiaromaticity relief.

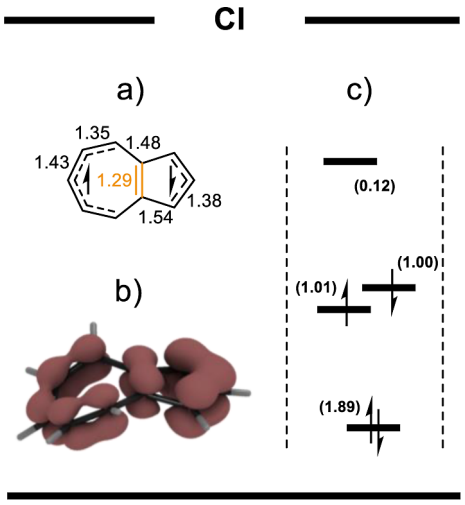

Figure 5. Summary of properties of the S_1 CASSCF(10,10) wave functions of the S_1−S_0 conical intersection of azulene, calculated in the S_1 state; (a) scheme of the proposed electronic structure and the bond lengths of CI azulene, (b) $EDDB_H$ plot, (c) canonicalized active-space natural MOs [reduced to (4,4) for clarity], their normalized occupancy (in brackets), and scheme of the dominant configuration.

3. CONCLUSIONS

In conclusion, the (anti)aromaticity of the lowest three singlet states of azulene (S_0, S_1, and S_2) explains its anti-Kasha behavior. Azulene is aromatic in its ground state, antiaromatic in its S_1, and aromatic in the S_2. The (anti)aromaticity of each state matches its lifetime, as experimentally determined by transient absorption spectroscopy (Figure 6 and Chapter S11). Moreover, the S_1 azulene's geometry relaxes significantly to alleviate its antiaromaticity. Consequently, the S_1 minimum-energy geometry of azulene is found near a conical intersection.

In the antiaromatic, S_1 minimum-energy geometry, azulene readily undergoes a favorable, nonradiative transition to its aromatic ground state through a conical intersection (Figure 6A). The depletion of S_1 through the conical intersection provides unimolecular antiaromaticity relief. By contrast, the aromatic S_2 is stabilized, does not undergo significant geometric relaxation, and maintains at high energy, which

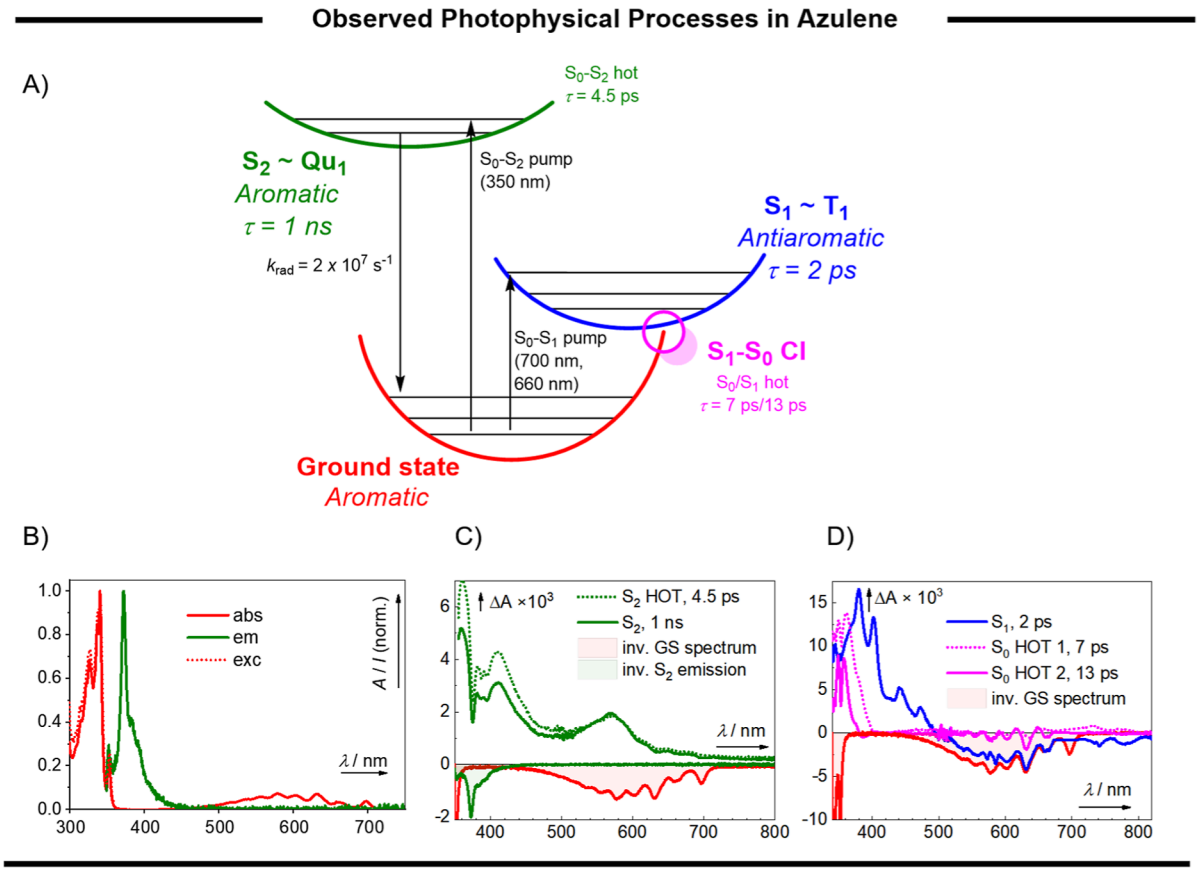

Figure 6. (Anti)aromaticity of the lowest three singlet states of azulene (S_0, S_1, and S_2) explains its anti-Kasha behavior. (A) Jablonski diagram of the experimentally observed photophysical phenomena, (B) UV−vis absorption, emission (λ_{exc} = 338 nm), and excitation spectra (λ_{em} = 372 nm) of azulene, (C) species associated spectra (SAS) of azulene excited at 350 nm (E = 600 nJ), and (D) SAS of azulene excited at 700 nm (E = 2 μJ). All spectra were recorded in cyclohexane.

https://doi.org/10.1021/jacs.3c07625
J. Am. Chem. Soc. 2023, 145, 21569−21575

causes a low rate of S_2-S_1 IC. For this reason, the S_2 state of azulene is long-lived and emitting, breaking Kasha's rule.

4. METHODS

Both PMO analysis[28] and Mandado's rules,[33] wherein π-electrons are separated by their spin (m), were extensively used in this study and supported by quantum chemical calculations of delocalization and aromaticity indices. We calculated HOMA,[37,38] MCI,[39] and FLU[40] and I_{ring}[41] indices for the C_5, C_7, and C_{10} circuits (Figure S6); in both "net" and "spin-separated" formulations, for all above states. We used the EDDB scheme, which represents electron delocalization that cannot be assigned to atoms or bonds due to its (multicenter) delocalized nature, to integrate the number of globally ($EDDB_G$ and $EDDB_H$) and locally ($EDDB_F$, $EDDB_E$, and $EDDB_P$) delocalized π-electrons[42,43] and, in particular, the density of delocalized π-electrons in the transannular bond of azulene (ΔC_{10}). Note that the spin-separated values of each index can be interpreted in line with Mandado's rules in open-shell systems. We also calculated the NICS[44] at the centroid of C_5 and C_7 fragments and constructed ACID[45] plots of S_0, T_1, and Qu_1 azulene and MRSCF MICD at CASSCF(10,10) level for S_0, S_1, and S_2.[34,35] ISE of methylated derivatives of S_0 and T_1 azulene were also calculated.[46] Full details on the computational methods and theoretical approach and the measured stationary absorption and emission and transient absorption spectra are provided in the Supporting Information.

■ ASSOCIATED CONTENT

Supporting Information

The Supporting Information is available free of charge at https://pubs.acs.org/doi/10.1021/jacs.3c07625.

PMO theory and Mandado's rules, computational methods, ground and excited state aromaticity calculations, S_1-S_0 conical intersection, NICS, dipole moment, ISE, ACID, MICD calculations, absorption and emission spectroscopy, time-resolved spectroscopy, and azulene versus naphthalene and homoazulene (PDF)

Optimized geometries (ZIP)

■ AUTHOR INFORMATION

Corresponding Authors

Henrik Ottosson − *Department of Chemistry—Ångström Laboratory, Uppsala University, Uppsala 751 20, Sweden;* orcid.org/0000-0001-8076-1165; Email: henrik.ottosson@kemi.uu.se

Tomáš Slanina − *Institute of Organic Chemistry and Biochemistry of the Czech Academy of Sciences, Prague 6 160 00, Czech Republic;* orcid.org/0000-0001-8092-7268; Email: tomas.slanina@uochb.cas.cz

Authors

David Dunlop − *Institute of Organic Chemistry and Biochemistry of the Czech Academy of Sciences, Prague 6 160 00, Czech Republic; Department of Inorganic Chemistry, Faculty of Science, Charles University in Prague, Prague 2 128 40, Czech Republic;* orcid.org/0000-0001-5351-7036

Lucie Ludvíková − *Institute of Organic Chemistry and Biochemistry of the Czech Academy of Sciences, Prague 6 160 00, Czech Republic*

Ambar Banerjee − *Division of X-ray Photon Science, Department of Physics and Astronomy—Ångström Laboratory, Uppsala University, Uppsala 751 20, Sweden*

Complete contact information is available at: https://pubs.acs.org/10.1021/jacs.3c07625

Author Contributions

All authors have given approval to the final version of the manuscript.

Funding

This research was funded by the INTER-COST grant (no. LTC20076) provided by the Czech Ministry of Education, Youth and Sports (D.D., L.L., and T.S.), and the Charles University Grant Agency project no. 379321 (D.D.). A.B. acknowledges funding from the Carl Tryggers Foundation (contract CTS 19:399). H.O. acknowledges the Swedish Research Council (Vetenskapsrådet) for financial support (grant 2019-05618). The computations were enabled by resources provided by the Swedish National Infrastructure for Computing (SNIC) at UPPMAX, which is partially funded by the Swedish Research Council through grant agreement no. 2021-22968.

Notes

The authors declare no competing financial interest.

■ ACKNOWLEDGMENTS

The authors thank Dr. Aleš Machara for initiating our interest in azulene chemistry and other anti-Kasha fluorophores, Dr. Carlos V. Melo for editing the paper and Nathalie Proos Vedin for her kind introduction to many of the computational methods applied herein.

■ REFERENCES

(1) Kasha, M. Characterization of Electronic Transitions in Complex Molecules. *Discuss. Faraday Soc.* **1950**, *9* (0), 14−19.

(2) Demchenko, A. P.; Tomin, V. I.; Chou, P.-T. Breaking the Kasha Rule for More Efficient Photochemistry. *Chem. Rev.* **2017**, *117* (21), 13353−13381.

(3) del Valle, J. C.; Catalán, J. Kasha's Rule: a Reappraisal. *Phys. Chem. Chem. Phys.* **2019**, *21* (19), 10061−10069.

(4) Behera, S. K.; Park, S. Y.; Gierschner, J. Dual Emission: Classes, Mechanisms, and Conditions. *Angew. Chem., Int. Ed.* **2021**, *60* (42), 22624−22638.

(5) Beer, M.; Longuet-Higgins, H. C. Anomalous Light Emission of Azulene. *J. Chem. Phys.* **1955**, *23* (8), 1390−1391.

(6) Binsch, G.; Heilbronner, E.; Jankow, R.; Schmidt, D. On the Fluorescence Anomaly of Azulene. *Chem. Phys. Lett.* **1967**, *1* (4), 135−138.

(7) Murata, S.; Iwanaga, C.; Toda, T.; Kokubun, H. Fluorescence Yields of Azulene Derivatives. *Chem. Phys. Lett.* **1972**, *13* (2), 101−104.

(8) Klein, R. F. X.; Horak, V. New Synthesis and Spectroscopic Studies of Thialene (Cyclopenta[b]thiapyran). *J. Org. Chem.* **1986**, *51* (24), 4644−4651.

(9) Liu, R. S. H.; Asato, A. E. Tuning the Color and Excited State Properties of the Azulenic Chromophore: NIR Absorbing Pigments and Materials. *J. Photochem. Photobiol., C* **2003**, *4* (3), 179−194.

(10) Viswanath, G.; Kasha, M. Confirmation of the Anomalous Fluorescence of Azulene. *J. Chem. Phys.* **1956**, *24* (3), 574−577.

(11) Kitai, J.-i.; Kobayashi, T.; Uchida, W.; Hatakeyama, M.; Yokojima, S.; Nakamura, S.; Uchida, K. Photochromism of a Diarylethene Having an Azulene Ring. *J. Org. Chem.* **2012**, *77* (7), 3270−3276.

(12) Murai, M.; Ku, S.-Y.; Treat, N. D.; Robb, M. J.; Chabinyc, M. L.; Hawker, C. J. Modulating Structure and Properties in Organic Chromophores: Influence of Azulene as a Building Block. *Chem. Sci.* **2014**, *5* (10), 3753−3760.

(13) Xin, H.; Li, J.; Lu, R.-Q.; Gao, X.; Swager, T. M. Azulene-Pyridine-Fused Heteroaromatics. *J. Am. Chem. Soc.* **2020**, *142* (31), 13598−13605.

(14) Xin, H.; Li, J.; Yang, X.; Gao, X. Azulene-Based BN-Heteroaromatics. *J. Org. Chem.* **2020**, *85* (1), 70−78.

(15) Dual fluorescence of multiple azulene derivatives was reported by Eber et al.[16] Most of the derivatives prepared in this study were also reported by Murata et al., who, unlike Eber et al., provided the quantum yields of S_2 emission.[7] However, according to Murata, the derivatives did not emit from S_1 or S_2, contradicting Eber et al. Upon further investigation of this discrepancy, we deduced that Eber et al. did not actually sensitize S_1 emission in azulene by substitution. Instead, they decreased the quantum yield of S_2 emission to QY = 10^{-5} or less, which was the detection limit reported by Murata et al. In the study by Eber et al., at low temperatures (77 and 4 K), the S_1 and S_2 emission intensities were similar. Thus, the quantum yield of S_1 emission of Eber et al.'s azulene derivatives was virtually identical to that of unsubstituted azulene, previously derived by gas-phase spectroscopy.[17]

(16) Eber, G.; Grüneis, F.; Schneider, S.; Dörr, F. Dual Fuorescence Emission of Azulene Derivatives in Solution. *Chem. Phys. Lett.* **1974**, *29* (3), 397−404.

(17) Huppert, D.; Jortner, J.; Rentzepis, P. M. Laser Excited Emission Spectroscopy of Azulene in the Gas Phase. *J. Chem. Phys.* **1972**, *56* (10), 4826−4833.

(18) Bearpark, M. J.; Bernardi, F.; Clifford, S.; Olivucci, M.; Robb, M. A.; Smith, B. R.; Vreven, T. The Azulene S_1 State Decays via a Conical Intersection: A CASSCF Study with MMVB Dynamics. *J. Am. Chem. Soc.* **1996**, *118* (1), 169−175.

(19) Baird, N. C. Quantum Organic Photochemistry. II. Resonance and Aromaticity in the Lowest $^3\pi\pi^*$ State of Cyclic Hydrocarbons. *J. Am. Chem. Soc.* **1972**, *94* (14), 4941−4948.

(20) Rosenberg, M.; Dahlstrand, C.; Kilså, K.; Ottosson, H. Excited State Aromaticity and Antiaromaticity: Opportunities for Photophysical and Photochemical Rationalizations. *Chem. Rev.* **2014**, *114* (10), 5379−5425.

(21) Solà, M. Aromaticity rules. *Nat. Chem.* **2022**, *14* (6), 585−590.

(22) Yan, J.; Slanina, T.; Bergman, J.; Ottosson, H. Photochemistry Driven by Excited-State Aromaticity Gain or Antiaromaticity Relief. *Chem.—Eur. J.* **2023**, *29* (19), No. e202203748.

(23) Minkin, V. I.; Glukhovtsev, M. N.; Simkin, B. Y. *Aromaticity and Antiaromaticity*; John Wiley & Sons, Incorporated, 1994.

(24) Balaban, A. T.; Oniciu, D. C.; Katritzky, A. R. Aromaticity as a Cornerstone of Heterocyclic Chemistry. *Chem. Rev.* **2004**, *104* (5), 2777−2812.

(25) Möllerstedt, H.; Piqueras, M. C.; Crespo, R.; Ottosson, H. Fulvenes, Fulvalenes, and Azulene: Are They Aromatic Chameleons? *J. Am. Chem. Soc.* **2004**, *126* (43), 13938−13939.

(26) Soncini, A.; Fowler, P. W. Ring-Current Aromaticity in Open-Shell Systems. *Chem. Phys. Lett.* **2008**, *450* (4−6), 431−436.

(27) Robertson, J. M.; Shearer, H. M. M.; Sim, G. A.; Watson, D. G. The Crystal and Molecular Structure of Azulene. *Acta Crystallogr.* **1962**, *15* (1), 1−8.

(28) Dewar, M. J. S.; Dougherty, R. C. PMO Treatment of Conjugated Systems. In *The PMO Theory of Organic Chemistry*; Dewar, M. J. S., Dougherty, R. C., Eds.; Springer US: Boston, MA, 1975, pp 73−130.

(29) Poater, J.; Heitkämper, J.; Poater, A.; Maraval, V.; Chauvin, R. Zwitterionic Aromaticity on Azulene Extrapolated to carbo-Azulene. *Eur. J. Org Chem.* **2021**, *2021* (46), 6450−6458.

(30) Scott, L. T.; Brunsvold, W. R.; Kirms, M. A.; Erden, I. Homoazulene. *J. Am. Chem. Soc.* **1981**, *103* (17), 5216−5220.

(31) Solà, M. Forty Years of Clar's Aromatic π-Sextet Rule. *Front. Chem.* **2013**, *1*, 22.

(32) El Bakouri, O.; Szczepanik, D. W.; Jorner, K.; Ayub, R.; Bultinck, P.; Solà, M.; Ottosson, H. Three-Dimensional Fully π-Conjugated Macrocycles: When 3D-Aromatic and When 2D-Aromatic-in-3D? *J. Am. Chem. Soc.* **2022**, *144* (19), 8560−8575.

(33) Mandado, M.; Grana, A. M.; Perez-Juste, I. Aromaticity in Spin-Polarized Systems: Can Rings Be Simultaneously alpha Aromatic and Beta Antiaromatic? *J. Chem. Phys.* **2008**, *129* (16), 164114.

(34) Pathak, S.; Bast, R.; Ruud, K. Multiconfigurational Self-Consistent Field Calculations of the Magnetically Induced Current Density Using Gauge-Including Atomic Orbitals. *J. Chem. Theory Comput.* **2013**, *9* (5), 2189−2198.

(35) Banerjee, A.; Halder, D.; Ganguly, G.; Paul, A. Deciphering the Cryptic Role of a Catalytic Electron in a Photochemical Bond Dissociation Using Excited State Aromaticity Markers. *Phys. Chem. Chem. Phys.* **2016**, *18* (36), 25308−25314.

(36) Michl, J.; Thulstrup, E. W. Why is Azulene Blue and Anthracene White? A Simple MO Picture. *Tetrahedron* **1976**, *32* (2), 205−209.

(37) Kruszewski, J.; Krygowski, T. M. Definition of Aromaticity Basing on the Harmonic Oscillator Model. *Tetrahedron Lett.* **1972**, *13* (36), 3839−3842.

(38) Krygowski, T. M. Crystallographic Studies of Inter- and Intramolecular Interactions Reflected in Aromatic Character of π-Electron Systems. *J. Chem. Inf. Comput. Sci.* **1993**, *33* (1), 70−78.

(39) Bultinck, P.; Ponec, R.; Van Damme, S. Multicenter Bond Indices As a New Measure of Aromaticity in Polycyclic Aromatic Hydrocarbons. *J. Phys. Org. Chem.* **2005**, *18* (8), 706−718.

(40) Matito, E.; Duran, M.; Solà, M. The Aromatic Fluctuation Index (FLU): A New Aromaticity Index Based on Electron Delocalization. *J. Chem. Phys.* **2004**, *122* (1), 014109.

(41) Giambiagi, M.; de Giambiagi, M. S.; dos Santos Silva, C. D.; de Figueiredo, A. P. Multicenter Bond Indices As a Measure of Aromaticity. *Phys. Chem. Chem. Phys.* **2000**, *2* (15), 3381−3392.

(42) Szczepanik, D. W.; Andrzejak, M.; Dominikowska, J.; Pawełek, B.; Krygowski, T. M.; Szatylowicz, H.; Solà, M. The Electron Density of Delocalized Bonds (EDDB) Applied for Quantifying Aromaticity. *Phys. Chem. Chem. Phys.* **2017**, *19* (42), 28970−28981.

(43) Szczepanik, D. W. A New Perspective on Quantifying Electron Localization and Delocalization in Molecular Systems. *Comput. Theor. Chem.* **2016**, *1080*, 33−37.

(44) Acke, G.; Van Damme, S.; Havenith, R. W. A.; Bultinck, P. Interpreting the Behavior of the $NICS_{zz}$ by Resolving in Orbitals, Sign, and Positions. *J. Comput. Chem.* **2018**, *39* (9), 511−519.

(45) Herges, R.; Geuenich, D. Delocalization of Electrons in Molecules. *J. Phys. Chem. A* **2001**, *105* (13), 3214−3220.

(46) Zhu, J.; An, K.; Schleyer, P. v. R. Evaluation of Triplet Aromaticity by the Isomerization Stabilization Energy. *Org. Lett.* **2013**, *15* (10), 2442−2445.

https://doi.org/10.1021/jacs.3c07625
J. Am. Chem. Soc. 2023, 145, 21569−21575